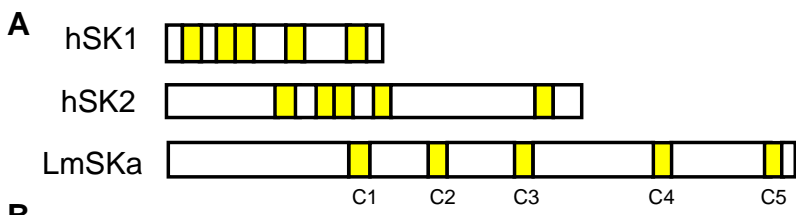


**Figure S1. SL metabolism in *Leishmania*.** Serine, CO<sub>2</sub>, and part of ethanolamine phosphate (EtN-P) are shown in green to illustrate the conversion. Abbreviations for enzymes (shown in circles): SPT, serine palmitoyltransferase; SK, sphingosine kinase; SPP, sphingosine-1-phosphate phosphatase; SPL, sphingosine-1-phosphate lyase; IPCS, IPC synthase; ISCL, inositol phosphosphingolipid phospholipase C-like protein. Abbreviations for metabolites: DHS, dihydrosphingosine; Sph, sphingosine; DHS1P, dihydrosphingosine-1-phosphate; S1P, sphingosine-1-phosphate; DH-cer, dihydroceramide; Cer, ceramide; IPC, inositol phosphorylceramide; SM, sphingomyelin; MYR, myriocin (an inhibitor of SPT); EtN-P, ethanolamine-phosphate; PE: phosphatidylethanolamine.



**B**

hsk1	-----		
hsk2	-----		
SKA	MHSLSSNNTSPHPATHRHTNHSSHTSSLLPPTASPVLQASCMSAKEDHIGADAQGIPS	60	
hsk1	-----		
hsk2	-----MAPPPLAASTPLLHGFEFGSYPARGPRFALTLTS-----	35	
SKA	SALFTP KPRIFAVPASTESPSPGATCHHAPTGGINVSAAATGVSAAHSDSGSNTAAPT	120	
hsk1	-----	MDPAGGPRG-----	9
hsk2	-----	-----QALHIQRLRPKPEARPRGGLVPLAEVSGCCTLRSR	70
SKA	SSSSPALQKQPPEHCYPAAYRGKLDAPHAVDDNMEAVILSKGRICTLAYFSPRGSFRIT	180	
hsk1	-----		
hsk2	SPSDSAAYFCIYTYPRGRGARRRATRTFRADGAATYEENRAEQRWATALTCLLRGLPL	130	
SKA	HVSSNGKTRVFNIPVRMIINIETAERDARQARQANDDTIKLVFAESGRNTRSLLCSF	240	
hsk1	-----	VLPRPC-----	15
hsk2	PG-----	-----DGEITPDLLPRPP-----	145
SKA	PSGAGEDNEGVLAVSVNTASLTLSSLGGPPTTASHFGAHTAACAAATAAPSIRYVH	300	
hsk1	-----		
hsk2	-----	RVLVLLNPRGGKKA	32
SKA	YVQRNKENPSIRTLEFQSSGPAETVQHVSTVQVHIYQKGSKHIIAFISAKSGKGEH	162	<b>C1</b>
hsk1	LFRSHVQPLLAEEAISFTLMLTERRNHARELVRSEE--LGRWDALVVM	SGDGLMHEVVNG	90
hsk2	WCKNHVLP MISEAGLSFNLIQTERQNHARELVQGLS--LSEWDGIVTV	SGDGLLHEVLNG	220
SKA	IFEKHVRPLLFHRSRHYQAHVTRRAHDCEDEVANLENPMDSENTVIAAV	GGDGMHETVNG	420
hsk1	LMER-----		100
hsk2	LLDR-----		230
SKA	VHRRKALVLRWLSVTANVSTGNGSVVSPDL SVHLNEERCAAVLLKSGSANKV VHHGEAS	480	
hsk1	IQKP-----		109
hsk2	VKMP-----		239
SKA	VDSPSPFIELGCEENKRDYGGNGVTPSAEATAREAYRLARCLVQGGWDALMPLVATVA	540	
hsk1	AGSGNALAASLNHYAGYEQVTNEDLLTNCTLLCRLLSPMN-----	LLSLHTASG	160
hsk2	CGSGNALAGAVNQHGGFEPALGLDLLNCSLLCRGGGHPD-----	LLSVTLASG	290
SKA	TGSACGLAKSLDVL SVTEAALS VHLSTVHMDLLLNFTPNEDMVEFHRCRMSRRLDA	600	<b>C3</b>
hsk1	LRLFS-----		165
hsk2	SRCFS-----		295
SKA	QREFSR YKEDKAAELQERSRLGEAPQLPRTLTAADCMTPFLKDGSNVYRDAVSCAMRMP	660	
hsk1	-----	VLSLAWGFIADVLDLESEKYRRLGEMRFTLG	214
hsk2	-----	FLSVAGWFVSDVDIQSERFRALG SARFTLG	347
SKA	ELHSRVAFM SLSFGSANDIDHGSESLRWGNARFQVYGGYMLRGLKRYKGLRYPWGS	720	<b>C4</b>
hsk1	-----		219
hsk2	EPASPTPAHSLPRAKSELTLTPDPAPPMAHSP LHRVSDLP LPLPQPALASPGSPEPLPI	407	
SKA	KAG--KTVEK LHRCKMPSTDDFPLCTMRESCPHCRQYVFVHC GAPLS SSIQGDTHPG	777	
hsk1	-----	SKTPASPVVVQQ-----	231
hsk2	LSLNGGPELAGDWGGAGDAPLSPDPLLSPPGSPKAAALHSPVSEGAPIPPSSGLPLPT	467	
SKA	-----	PTPNTSRSTAQPISAAEVLAP-----	798
hsk1	-----	GPVDAHLVPLEEPVPSHWTVVDEDFVLV LALLHSHLGSEMFAAPMGRC	281
hsk2	PDARVGASTCGPPDHLLPPLGTPLPPDWVTLEG-DFVLM LAISPSHLGADLVAAPHARFD	526	
SKA	-----	YTDQQLLDEEDVDFKDERLP-WVTVRG-DFCIALLCNVRDVAQDMLMAPLAHMS	850
hsk1	AGVMHLFYVRAG-----	VSRAMLLRLFLAMEKGRHMEYECPYLVYVPVAFRLEPKDGG	336
hsk2	DGLVHLCWVRSG-----	ISRAALLRFLAMERGSFSLGCPQLGYAAARAFRLEPLTRPG	581
SKA	DGAIDVYCRVDPI TGRGRMEMLKFVIGLES GSHVNLDFVNYVKARALEIKVD----	AG	906
hsk1	VFAVDGELMVSEAVQGVHPNYFWMVSGC VEPSPSWKPPQMPPEEPL	384	<b>C5</b>
hsk2	VLTVDGEQVEYGPLQAQMHPGIGTLT LG-----	PPGC-----	PGREP- 618
SKA	ISMSDGE LMP LSSVRVTKMRGSVQFVRS G-----		935

**Figure S2. Comparison of SKs from human and *L. major*.** (A) Schematic representation of human SK1 (NM\_001142601), human SK2 (AF245447), and *L. major* SKa (Tritypdb LmjF26.0710). Yellow boxes indicate the five conserved regions (C1-C5) found in all SKs. (B) ClustalW alignment of *L. major* SKa, human SK1 and human SK2. The underlined sequence (amino acid 343-421 of SKa) represents the predicted diacylglycerol kinase catalytic domain. Asterisks (\*): fully conserved residues; colons (:): highly similar residues; periods (.): weakly similar residues.

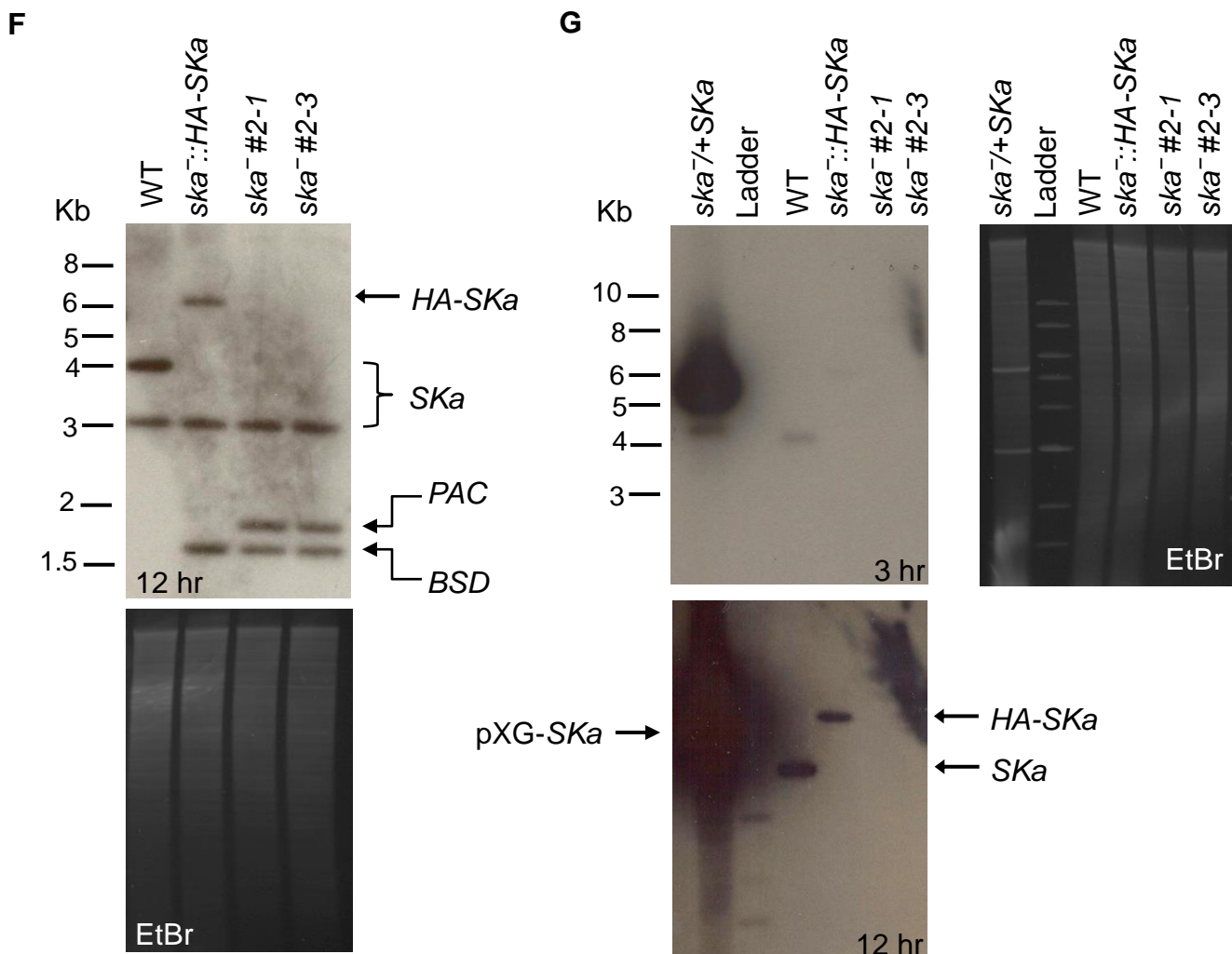
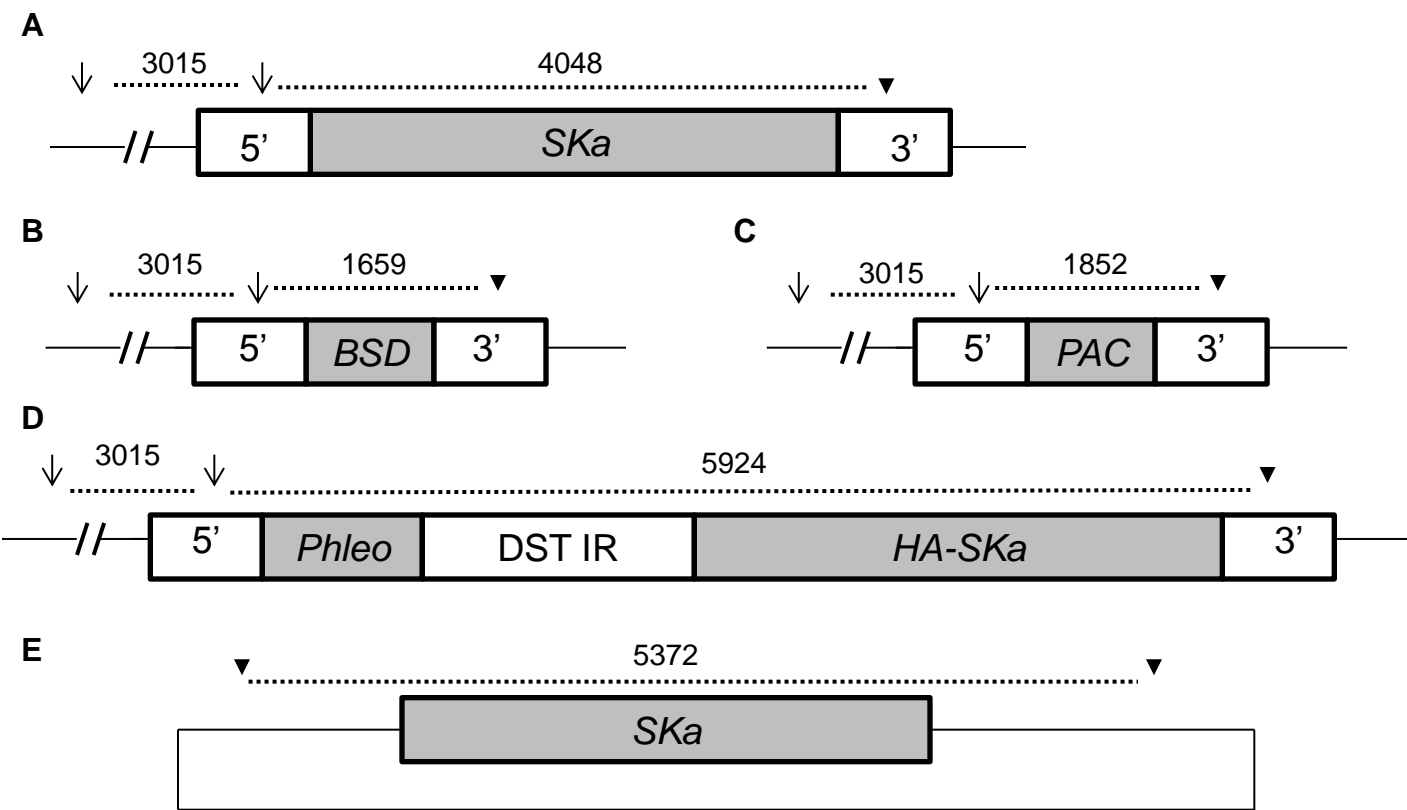


**Figure S3. Targeted deletion of *SKa* in *L. major*.** (A-E) Schematic representations of the WT *SKa* allele (A), the replacement of *SKa* with *BSD* (B) or *PAC* (C), the chromosomal knockin of *HA-SKa* (D), and the episomal expression of *SKa* from pXG-*SKa* (E). 5': Upstream flanking region; 3': downstream flanking region; DST IR: downstream intergenic region. (F-G) Southern blot analyses of genomic DNA digested with *EcoRI* (↓ in A-E) and *HindIII* (▼ in A-E). Blots were hybridized with the 5' probe (F) or the *SKa* ORF probe (G). Dotted lines in A-E indicate the expected fragment sizes in bp (not drawn to scale). Exposure times and DNA loading controls (EtBr staining) are included in F and G.

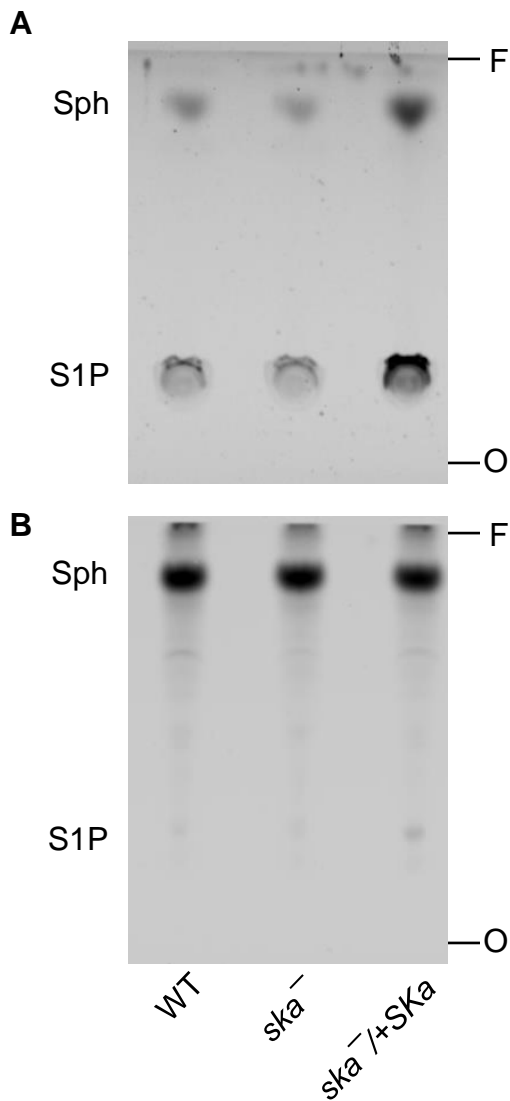


**Figure S4. SK activity in *L. major* promastigotes.** (A-B) Lysates from WT, *ska*<sup>-</sup>, or *ska*<sup>-</sup>/+SKa promastigotes were incubated with NBD-Sph as described in Experimental Procedures. After lipid extraction, each sample was partitioned into approximately equal volumes of aqueous phase and organic phase. 5  $\mu$ l of the aqueous phase (A) and 5  $\mu$ l of organic phase (B) from each sample were resolved by TLC. O: origin of migration; F: solvent front.

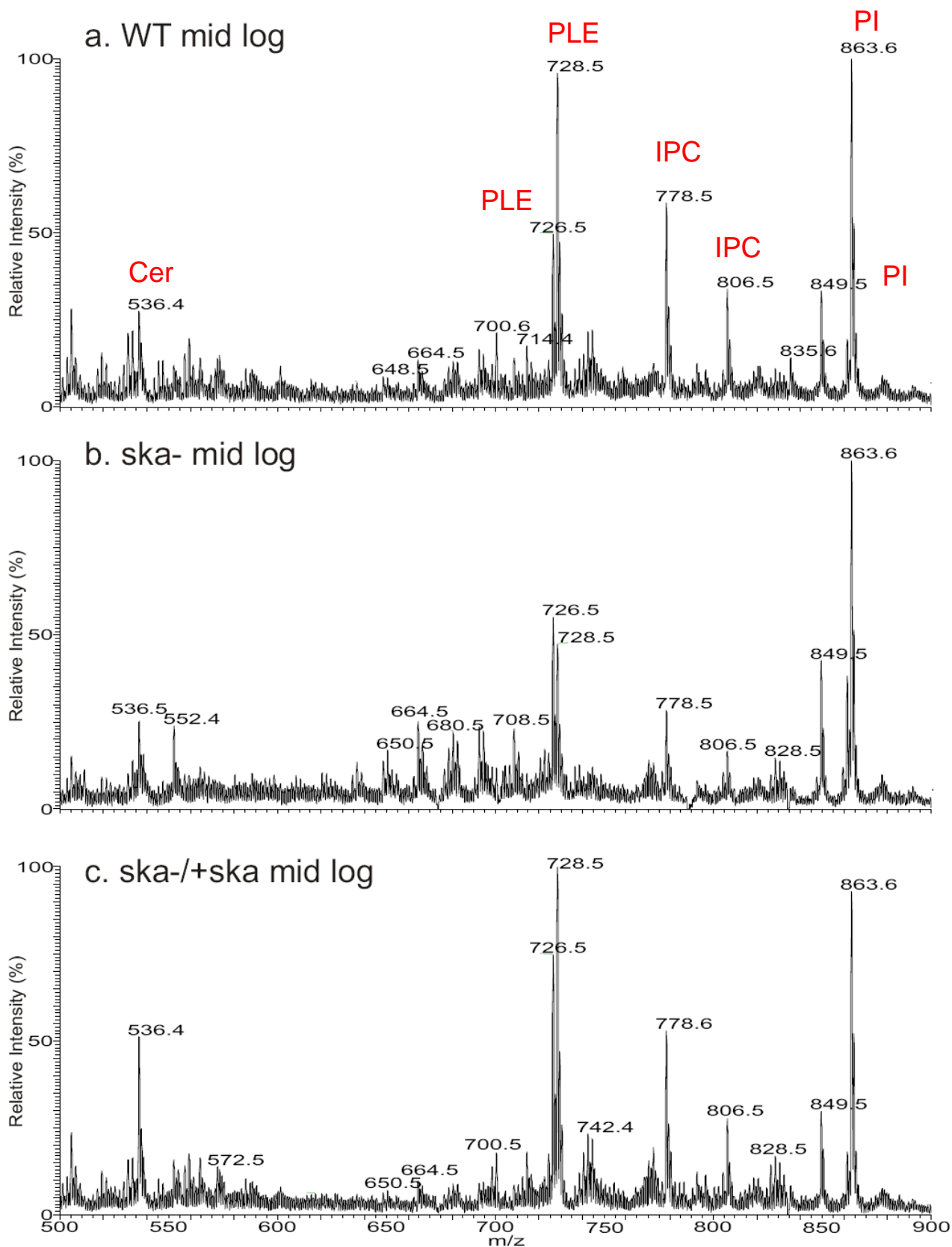


**Figure S5. Negative-ion ESI/MS spectra of total lipids from log phase promastigotes of WT (a), *ska*<sup>-</sup> (b), and *ska*<sup>-</sup>/*+SKa* (c). [M-H]<sup>-</sup> ions representing ceramide, PLE, IPC, and PI are labeled in red.**

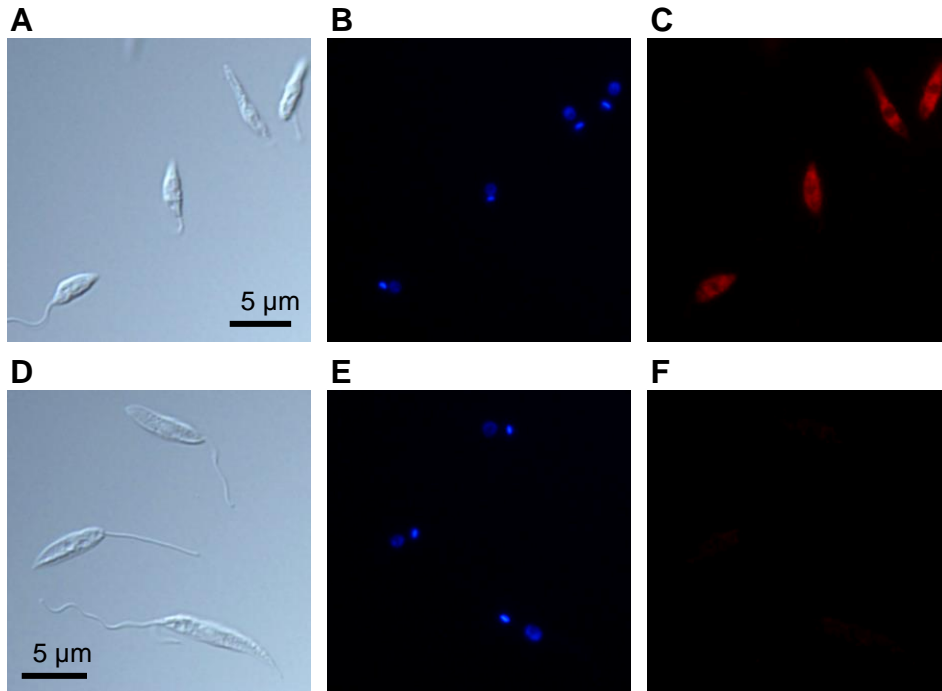


**Figure S6. Cytoplasmic localization of HA-SKa expressed from the endogenous locus of *SKa*.** Log phase promastigotes of *ska*<sup>-</sup>::*HA-SKa* (A-C) or *ska*<sup>-</sup> (D-F) were permeabilized and subjected to immunofluorescence microscopy. (A, D) Differential interference contrast images; (B, E) DNA staining with Hoechst 33242; (C, F) rabbit anti-HA polyclonal antibody labeling followed by incubation with a Texas Red-conjugated goat anti-rabbit IgG antibody.



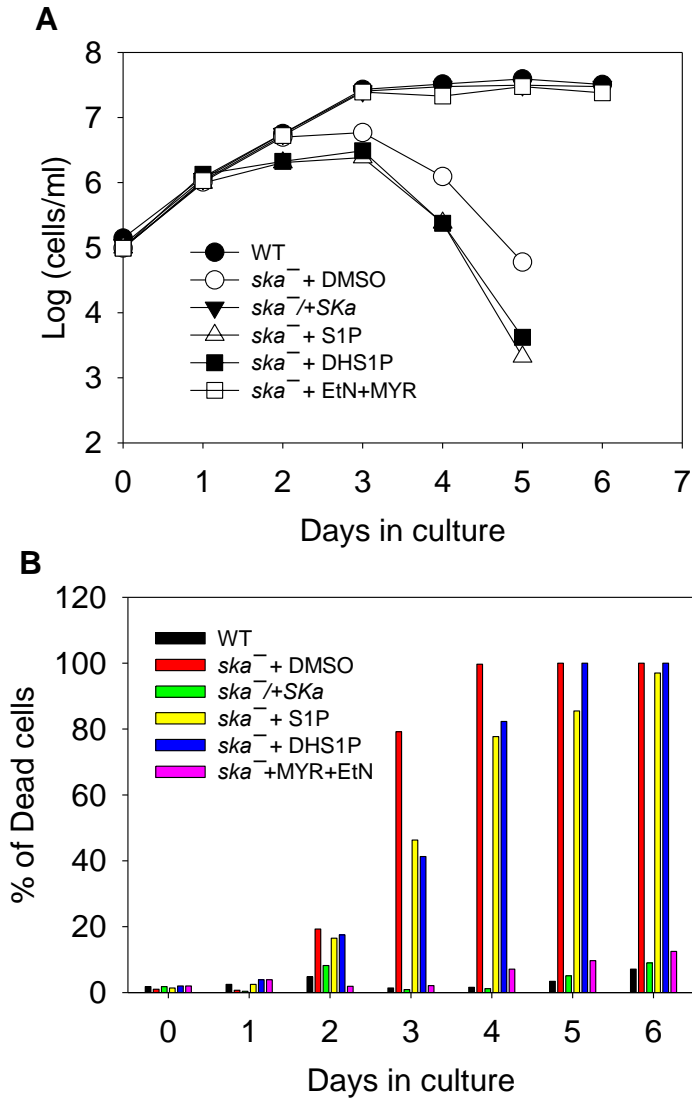


**Figure S7. S1P or DHS1P fail to reverse the growth defect of *ska*<sup>-</sup> mutants in culture.** Promastigotes were inoculated at  $1.0 \times 10^5$  cells/ml and incubated at 27 °C. Culture densities (**A**) and percentages of dead cells (**B**) were monitored daily. *Ska*<sup>-</sup> mutants were supplemented with S1P (2 μM), DHS1P (2 μM), EtN + MYR (200 μM and 1 μM, respectively), or 0.1% of DMSO (solvent control). Experiments were repeated three times and results from one representative set were shown here.

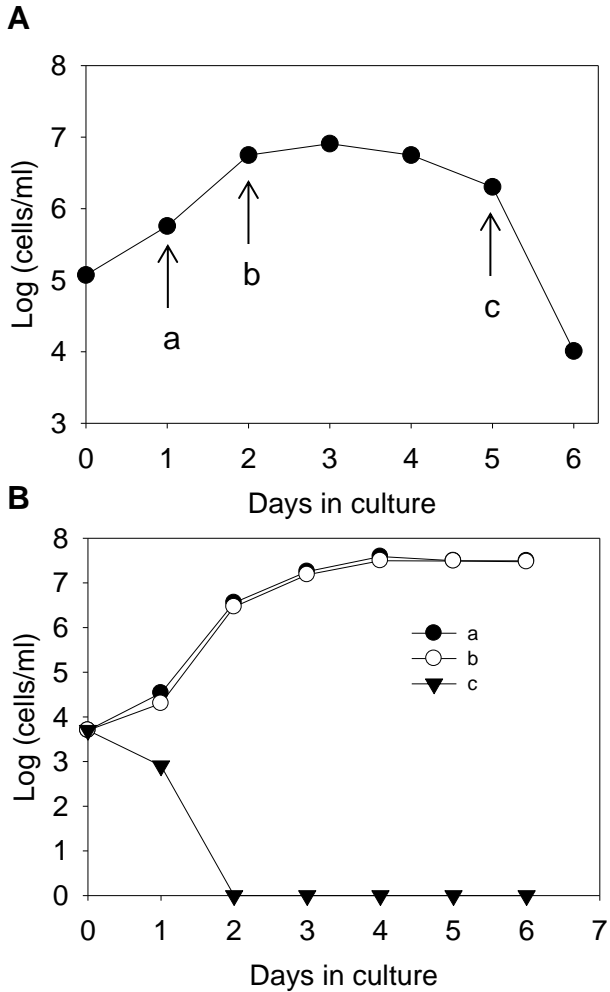


**Figure S8. *Ska*<sup>-</sup>-conditioned medium is toxic. (A)** *Ska*<sup>-</sup> promastigotes were inoculated in M199 medium at  $1.0 \times 10^5$  cells/ml and incubated at 27 °C (without MYR or EtN supplements). Culture densities were monitored daily. At day 1, 2, and 5, conditioned medium was collected by centrifugation (to remove cells) and designated as a, b, and c, respectively. **(B)** WT promastigotes were inoculated in *ska*<sup>-</sup>-conditioned medium (a, b, or c as indicated in **A**) at  $6 \times 10^3$  cell/ml. Culture densities were monitored daily. Experiments were repeated twice and results from one representative set were shown here.

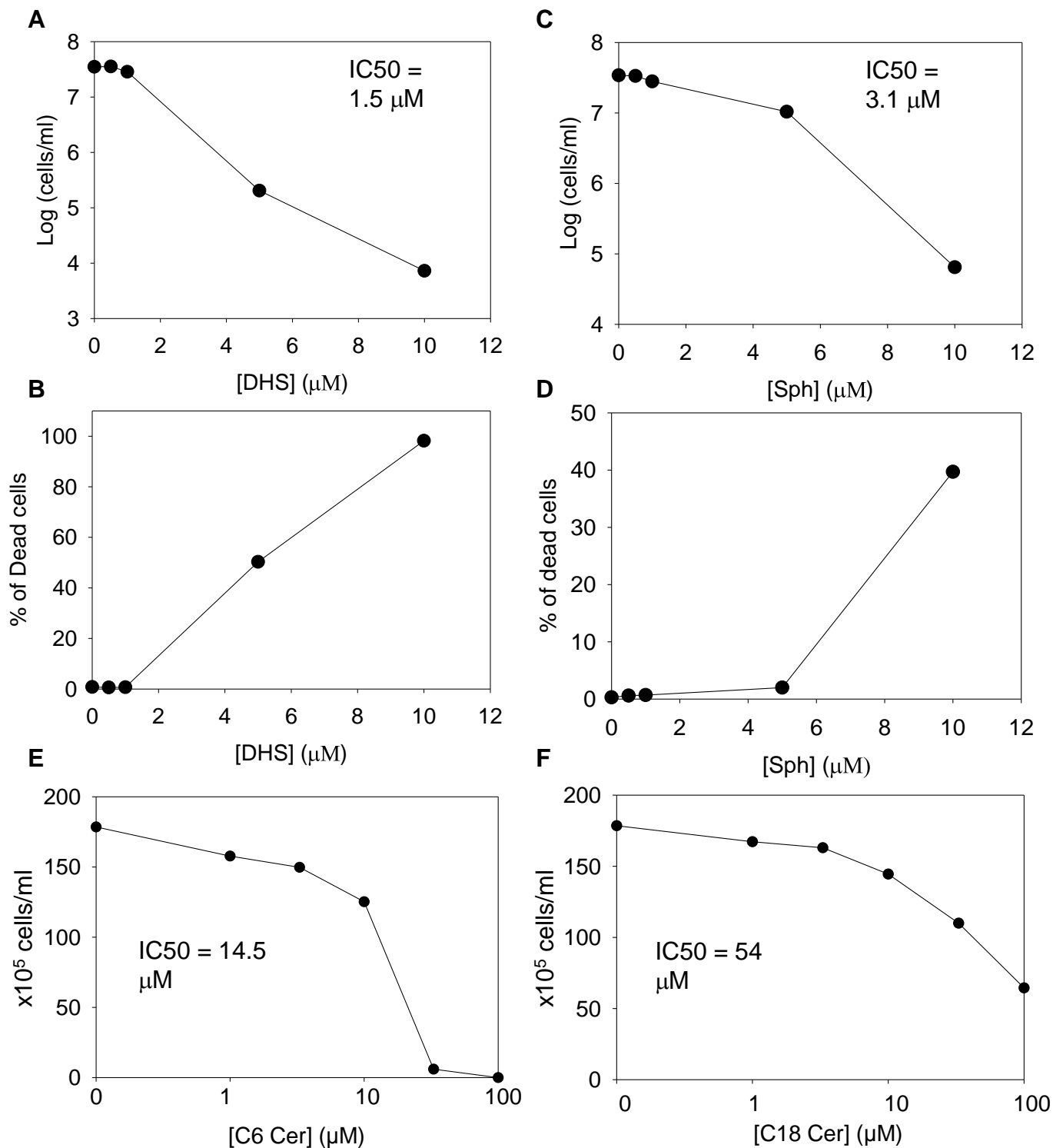


**Figure S9. Effects of exogenous sphingoid bases or ceramides on *L. major* promastigotes.** WT promastigotes were inoculated in 0-10  $\mu\text{M}$  of DHS (A-B), 0-10  $\mu\text{M}$  of Sph (C-D), 0-100  $\mu\text{M}$  of C6-ceramide (E), or 0-100  $\mu\text{M}$  of C18-ceramide (F) at  $2.0 \times 10^5$  cell/ml. Culture densities (A, C, E, and F) and percentages of dead cells (B, D) were determined after 48 hours. Experiments were repeated three times and results from one representative set were shown here. IC<sub>50</sub> values represent the concentrations required to inhibit growth by half.

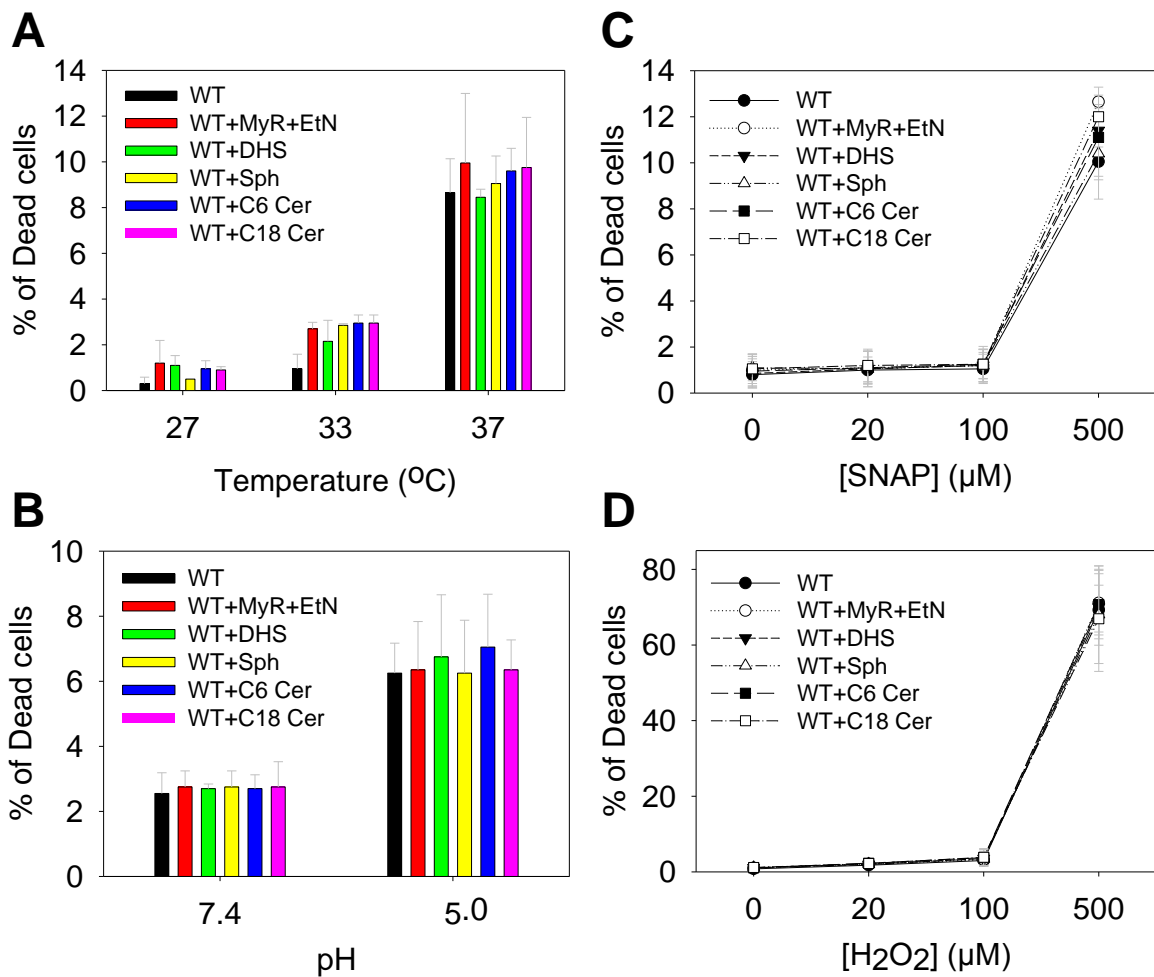


**Figure S10. WT promastigotes treated with sphingolipid metabolites are not hypersensitive to stress conditions.** (A-B) WT promastigotes were cultured under regular condition (27 °C, pH 7.4) to stationary phase before stress treatments. In **A**, parasites were transferred to 37 °C, 33 °C, or remained at 27 °C. In **B**, half of the parasites were transferred to an acidic medium (pH 5.0) while the other half remained in regular medium (pH 7.4) for 72 hours at 27 °C. (C-D) Stationary phase promastigotes were challenged with 0-500 μM of SNAP (C) or hydrogen peroxide (D). In these experiments, WT promastigotes were supplemented with MYR+EtN (1 μM and 200 μM, respectively), or 0.5 μM of DHS/Sph/C6 ceramide/C18 ceramide daily. Percentages of cell death were determined at 24 (A), 48 (C-D), or 72 (B) hours post treatments; and error bars indicate standard deviations from two independent repeats.

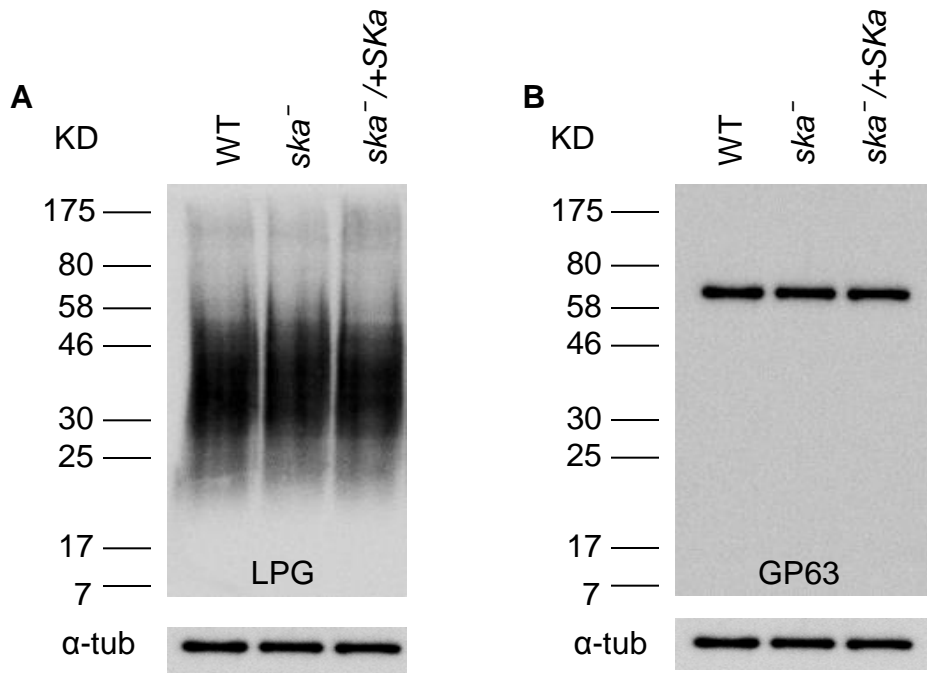


**Figure S11. Expression of LPG and GP63 is not altered in *ska*<sup>-</sup> mutants.** Whole cell lysates from stationary phase promastigotes were resolved by SDS-PAGE and transferred to PVDF membranes. Monoclonal antibodies WIC79.3 and 96-126 (Cedarlane Labs) were used to detect LPG (**A**) and GP63 (**B**), respectively. A monoclonal anti- $\alpha$ -tubulin antibody was used to control loading (bottom).

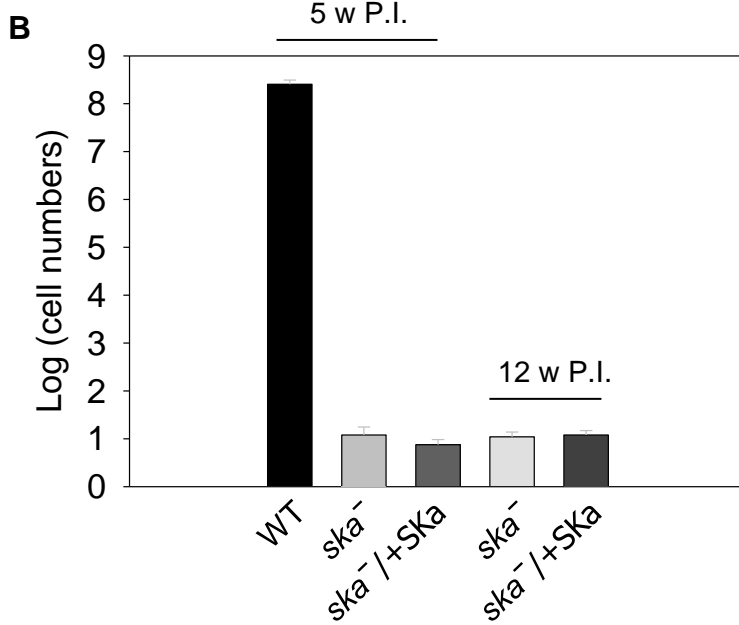
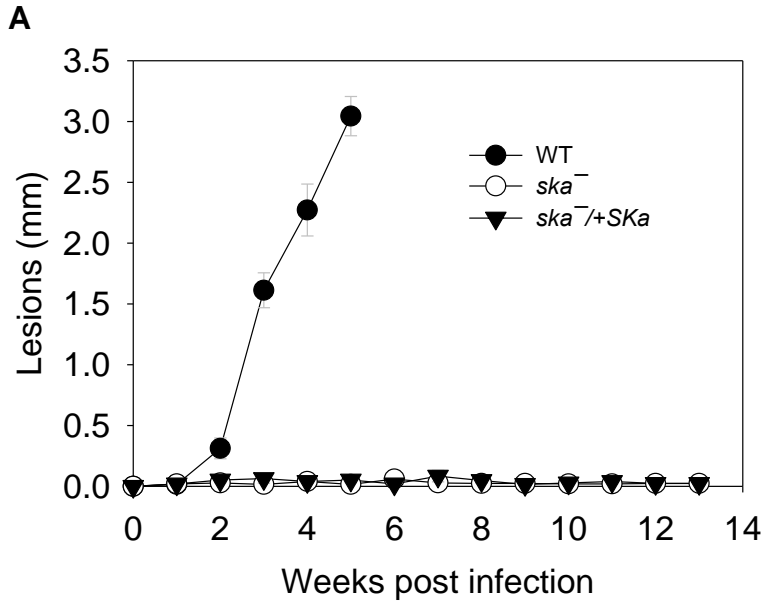


**Figure S12. Metacyclics of *ska*<sup>-</sup> and *ska*<sup>-</sup>/*+SKa* fail to induce pathology in BALB/c mice.** BALB/c mice were infected in the footpads with metacyclics ( $2.0 \times 10^5$  cells/mouse, 5 mice/group). (A) Lesion sizes of infected footpads were measured weekly with a caliper. (B) Parasite numbers in the infected footpads were determined at 5 or 12 weeks post infection (w P.I.) by limiting dilution assay. Error bars represent standard deviations.